Adsorption/reduction of *N*-dimethylnitrosamine from aqueous solution using nano zero-valent iron nanoparticles supported on ordered mesoporous silica

Xiaodong Xin, Shaohua Sun, Mingquan Wang, Qinghua Zhao, Yan Chen and Ruibao Jia

ABSTRACT

N-Dimethylnitrosamine (NDMA) has aroused increasing concern among public health agencies. It is necessary to develop some effective methods to remove NDMA from drinking water. A reductive process has been investigated as an alternative treatment method for NDMA removal from water. In this manuscript, zero-valent iron nanoparticles (ZVINPs) were synthesized, and then supported on mesoporous silica materials with high surface area (MCM-41) to prepare a stable ZVINP/MCM-41 nanocomposite. X-ray diffraction measurements showed the stabilization of the ZVINPs upon their support on MCM-41, which enhanced their activity. The ZVINP/MCM-41 nanocomposite was used for the catalytic reduction of NDMA in the model solution, and the results showed the dependency of the removal process on the ZVINP/MCM-41 mass, time of removal, and solution pH. The mechanism of NDMA reduction by ZVINP/MCM-41 was studied, and the results showed the conversion of NDMA to unsymmetrical dimethylhydrazine, dimethylamine (DMA) and NH_4^+. The product analysis found that in the process of removal, adsorption and reduction existed at the same time.

Key words | loaded type nano zero-valent iron, *N*-dimethylnitrosamine, product analysis, removal mechanism

Xiaodong Xin
Shaohua Sun
Mingquan Wang
Qinghua Zhao
Yan Chen
Ruibao Jia (corresponding author)
Jinan Water and Waste Water Monitoring Center,
Jinan 250021,
China;
Shandong Province City Water Supply and Drainage Water Quality Monitoring Center,
Jinan 250021,
China;
and
Shandong Water Treatment Engineering Technology Research Center,
Jinan 250021,
China
E-mail: *jiaruibao1968@163.com*

INTRODUCTION

As the National Toxicology Program reported in 2011, *N*-dimethylnitrosamine (NDMA) is reasonably anticipated to be a human carcinogen. It is detected in many drinking water sources and rivers in some countries (such as China, USA and Canada), and also in treated drinking water and waste water (Mitch *et al*. 2003; Han *et al*. 2013). Subsequent studies have demonstrated that NDMA is one disinfection by-product of chlorination and chloramination of water and waste water (Choi & Valentine 2002; Mitch & Sedlak 2002). Besides, it can be formed during ozonation and other treatments with strong oxidants (Andrzejewski *et al*. 2008; Yang *et al*. 2009; von Gunten *et al*. 2010). It arouses increasing concern among public health agencies. The US Environmental Protection Agency classifies it in group B2 as a 'Probable human carcinogen'. So it is necessary to develop some effective methods to remove it from drinking water.

Reductive processes with or without the augment of hydrogen have been investigated as alternative treatment methods for NDMA removal. Catalysts, including Pd, Pd-Cu, Pd-In, Ni and NiB, have shown the ability to reduce NDMA with hydrogen (Davie *et al*. 2008; Frierdich *et al*. 2009). Zero-valent iron and nickel-enhanced iron both transform NDMA to dimethylamine (DMA) and NH_4^+ without hydrogen (Odziemkowski *et al*. 2000). Like many other nanomaterials, the zero-valent iron nanoparticle (ZVINP) is easy to agglomerate into large particles, resulting in the decrease of surface area and reactivity performance,

doi: 10.2166/ws.2017.003

which limits its application in water treatment (Phenrat *et al.* 2006). Therefore, researchers have paid attention to the modification of nano zero-valent iron (He & Zhao 2005; Chun *et al.* 2010; Wang *et al.* 2010; Zhang *et al.* 2011). Immobilization of ZVINP in mesoporous material is a promising approach to solve the problem above (Li *et al.* 2011; Lv *et al.* 2011). Mesoporous materials with large specific surface area, uniform aperture adjustment, morphology and active surface groups come onto people's horizons. It is widely used in macromolecule adsorption and separation, biological medicine, chemical catalysis, chemical sensors, and the synthesis of nanomaterials (Wakayama *et al.* 2003; Fan *et al.* 2005). Mesoporous silica has attracted intense interest due to its adsorption capacity, high surface area, porous structure, and relatively low cost. Mesoporous silica MCM-41 has been proven to be generally quite effective for iron loading (Liu *et al.* 2014). The combination of MCM-41 and ZVINP would take advantage of the two materials. It is interesting to evaluate the efficiency of NDMA adsorption/reduction by ZVINP supported on MCM-41.

In this study, we designed and prepared a new kind of nanocomposite by loading nano zero-valent iron onto ordered mesoporous silica materials (ZVINP/MCM-41), which could reduce contact with oxygen. It could avoid zero-valent iron oxide and increase adsorption at the same time. The prepared ZVINP/MCM-41 showed excellent reductive performance towards NDMA.

EXPERIMENTAL

Materials and chemicals

All chemicals, obtained from Sinopharm Chemical Reagent Beijing Co Ltd, China, are of analytical reagent grade or better quality. Ultrapure water was used throughout the experiment (18.2 MΩ cm).

Synthesis of ZVINP/MCM-41

MCM-41 was synthesized according to the literature as by Dimos *et al.* (2009). An amount of 50 g tetraethylorthosilicate was added into a polyethylene bottle containing 417.5 g H_2O, 268.5 g NH_3 (25% wt) and 10.5 g cetyltrimethylammonium bromide, and stirred for 30 min. After heat treatment at 80 °C for 96 h, the product was retrieved. It was filtered, rinsed with cold ethanol and finally placed on a plate for air-drying.

ZVINP/MCM-41 was prepared by the liquid phase reduction method. Typically, $FeSO_4{\cdot}7H_2O$ (8.93 g) was dissolved in ethanol/water (4/6) solution (100 mL), followed by the addition of polyethylene glycol-4000 (0.125 g/g). MCM-41 (20 g) was added into the above solution and stirred well. Then, $NaBH_4$ solution (0.45 mol/L) was added into the above mixed solution drop by drop. All of the reactions were conducted in an anaerobic environment. After reaction, the products were washed three times with ethanol, acetone, and anaerobic water (oxygen was removed from the water by passing nitrogen through the water) respectively. The resulting precipitates (ZVINP/MCM-41) were ready for characterization.

Characterization

The morphological structure of ZVINP/MCM-41 was observed by ZEISS scanning electron microscopy. All SEM specimens were sputter-coated with a thin layer of gold palladium under vacuum in an argon atmosphere prior to examination. X-ray diffraction (XRD) patterns of the prepared samples were acquired with a Tokyo Rigaku D/MAX 2200 X-ray diffractometer using CuKα radiation (40 kV, 300 mA) of wavelength 0.154 nm to confirm the structure of the materials. Surface area measurements were performed on a Micromeritics ASAP 2020 surface area and porosity analyzer. Fourier transform infrared (FTIR) spectra were recorded in the spectral range of 4,000–400 cm^{-1} on a Perkin–Elmer Spectrum One FTIR spectrometer.

Batch experiment for NDMA adsorption/reduction

In a typical batch experiment, 20 mg of the as-prepared ZVINP/MCM-41 was added into a 1,000 mL 1.0 μg/L of NDMA solution, the mixture was adjusted to pH 7.6 using HCl and NaOH and stirred for 120 min. Thereafter, ZVINP/MCM-41 was separated by filter separation. In order to obtain the reaction kinetics of the NDMA solutions, different reaction times (15–240 min) were treated with the same procedure as above. In order to obtain the removal

isotherms of the NDMA solutions, varying initial concentrations of individual NDMA solutions (1.0–6.0 μg/L) were treated with the same procedure as above at room temperature. Blank samples (containing only deionized water and corresponding ZVINP/MCM-41) were prepared and monitored for the duration of the experiment as a control.

The removal efficiency and the amount of NDMA removed q (μg/g) were given according to the formula:

$$\text{Removal efficiency } (\%) = \frac{c_0 - c_t}{c_0} \times 100\% \quad (1)$$

$$q_t = \frac{(c_0 - c_t) \times V}{m} \quad (2)$$

where c_t (μg/L) is the concentration of NDMA at time t (min), V (L) is the volume of NDMA solution, m (g) is the mass of ZVINP/MCM-41, q_t (μg/g) is the removal amount at time t (min).

Analytical method

The NDMA in the solution was analyzed using an Agilent 7890A triple quadrupole gas chromatography–mass spectrometer. It was equipped with an HP-5MS column (30 m × 0.25 mm, 0.25 μm) using helium (99.999%) as carrier gas (1 mL/min flow rate). The column temperature was held at 40 °C for 1 min, increased to 150 °C at 5 °C/min, and then increased to 280 °C at 20 °C/min. Temperatures of the transfer line and source of ionization were 280 °C and 230 °C, respectively. The injection port temperature was 250 °C. The retention time of NDMA was 3.95 min.

For unsymmetrical dimethylhydrazine (UDMH) measurement, the liquid samples were pretreated by 4-nitrobenzaldehyde, separated by the C18 column and detected by the ultraviolet detector ($\lambda = 390$ nm). The acetonitrile and water with a volume ratio of 4:1 were taken as the mobile phases. DMA concentration was measured by an Agilent GC7890/FID after derivatization with benzenesulfonyl chloride using the improved method by Yang *et al.* (2010). It was equipped with an HP-5 column (30 m × 0.32 mm, 0.25 μm) using nitrogen (99.999%) as carrier gas (2 mL/min flow rate). The column temperature was held at 120 °C, increased to 195 °C at 40 °C/min, held for 1 min, and then increased to 290 °C at 60°C/min. The injection port temperature was 280 °C. The retention time of DMA was 6.56 min.

RESULTS AND DISCUSSION

Characterization of ZVINP/MCM-41

The surface morphology of MCM-41 and ZVINP/MCM-41 can be seen from Figure 1(a) and 1(b). Compared with Figure 1(a), after loading with nano zero-valent iron, a layer of spherical particles adhered to and was evenly distributed on the surface of the MCM-41, as shown in Figure 1(b).

The XRD patterns of MCM-41 and ZVINP/MCM-41 are presented in Figure 1(c) and 1(d). Figure 1(c) compares the X-ray diffraction patterns of MCM-41 before and after ZVINP loading. In Figure 1(c), there is an obvious zero-valent iron characteristic peak at $2\theta = 43°$–$45°$ (α-Fe^0), which is in accordance with the report by Choi & Valentine (2002). It indicates that ZVINP was successfully loaded into MCM-41.

The FTIR spectra of MCM-41 and ZVINP/MCM-41 in the range of 4,000–400 cm^{-1} are shown in Figure 1(d). A band at 3,445 cm^{-1} in the spectra shows H–O–H hydrogen-bonded water. The intensive band at around 1,040 cm^{-1} could be assigned to Si–O stretching vibrations. After loading ZVINP, the Fe–O and Fe–OH vibrations appeared at 1,400 and 1,020 cm^{-1}, respectively.

According to the Brunauer–Emmett–Teller (BET) analysis, after loading ZVINP, Barrett–Joyner–Halenda (BJH) desorption cumulative volume of pores was 0.1785 cm^3/g, which was smaller than that before loading ZVINP (0.2037 cm^3/g) and the BET surface area was 30.58 m^2/g, which was larger than that before loading ZVINP (27.64 m^2/g). This may be due to the loading of ZVINP on the surface of the MCM-41, which could increase the surface area.

Effect of operating variables on the removal of NDMA using ZVINP/MCM-41

Comparison of different materials on removal

Three kinds of materials, ZVINP, MCM-41, and ZVINP/MCM-41, were used based on the same mass to remove 1,000 mL 1.0 μg/L NDMA. Two-hour removal experiments were carried out. From Figure 2(a), it is clear that the adsorption capacity of ZVINP/MCM-41 was better than

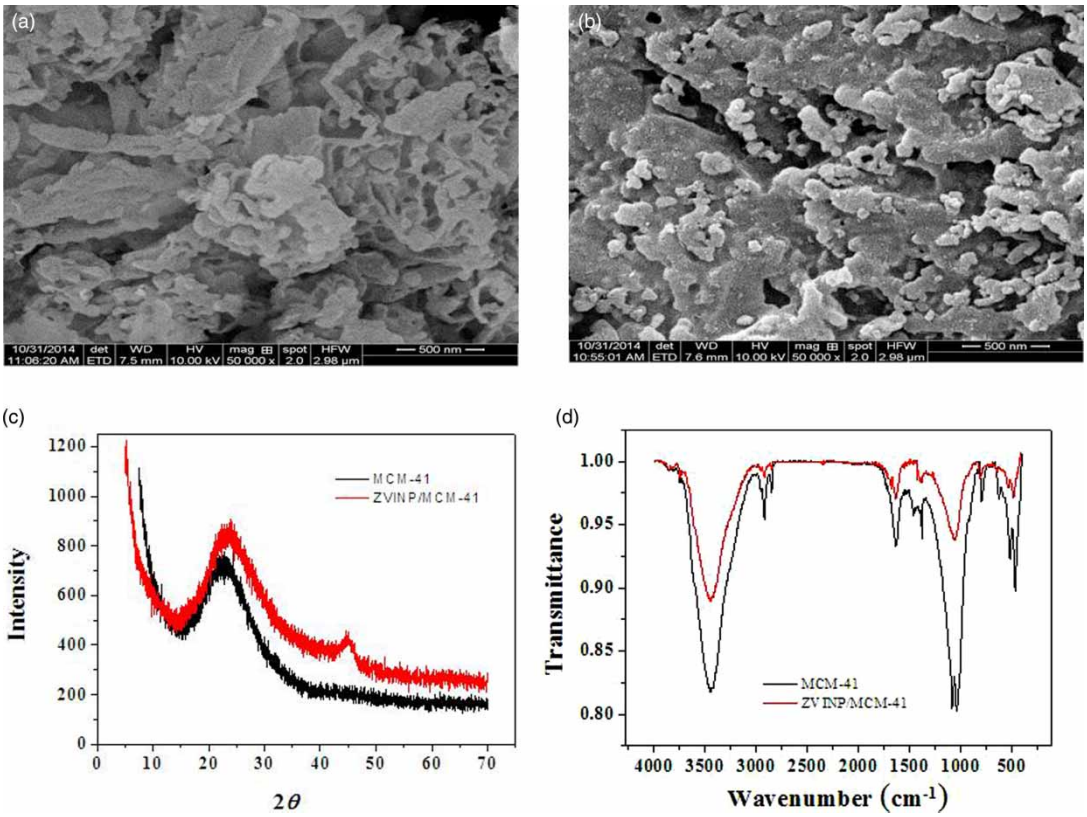

Figure 1 | Characterization of MCM-41 and ZVINP/MCM-41: (a) scanning electron microscopy of MCM-41; (b) scanning electron microscopy of ZVINP/MCM-41; (c) XRD diffraction pattern of MCM-41 (black line) and ZVINP/MCM-41 (red line); (d) FTIR of MCM-41 (black line) and ZVINP/MCM-41 (red line). Please refer to the online version of this paper to see this figure in colour: http://dx.doi.org/10.2166/ws.2017.003.

ZVINP and MCM-41. Therefore, ZVINP/MCM-41 was used to remove NDMA.

Effect of ZVINP/MCM-41 concentration

In order to determine the effect of ZVINP/MCM-41 dose, the 2 h removal experiments were carried out at 25°C within the ZVINP/MCM-41 dosage range from 5 to 40 mg in 1,000 mL 1.0 μg/L NDMA solution. As shown in Figure 2(b), the removal of NDMA increased with the increase of ZVINP/MCM-41 dose, and reached a plateau at the appropriate dose of 20 mg. A dose of 20 mg of the nanocomposite was chosen for the research.

Effect of initial pH

The pH value of the solution was an important controlling parameter in the removal process. To determine the effect of pH, the 2 h removal experiments were carried out at 25 °C with the pH ranging from 4.3 to 9.2 in 1,000 mL 1.0 μg/L NDMA solution. The removal of NDMA using ZVINP/MCM-41, ZVINP and MCM-41 increased significantly with increasing pH from 4.3 to 7.6, and decreased obviously at pH 9.2. It can be concluded that too much acid or alkaline could affect the structure of ZVINP/MCM-41, which may reduce the NDMA removal rate of ZVINP/MCM-41 (Figure 2(c)). Under pH 7.6, the removal efficiency of NDMA using ZVINP/MCM-41 was better.

The reaction time

A dose of 20 mg ZVINP/MCM-41 was added into 1,000 mL 1.0 μg/L (0.0135 mmol/L) of NDMA solution at pH 7.6 and the remaining amount of NDMA in solution was detected at 15, 30, 45, 60, 75, 90, 120, 150, 180, 210, and 240 min,

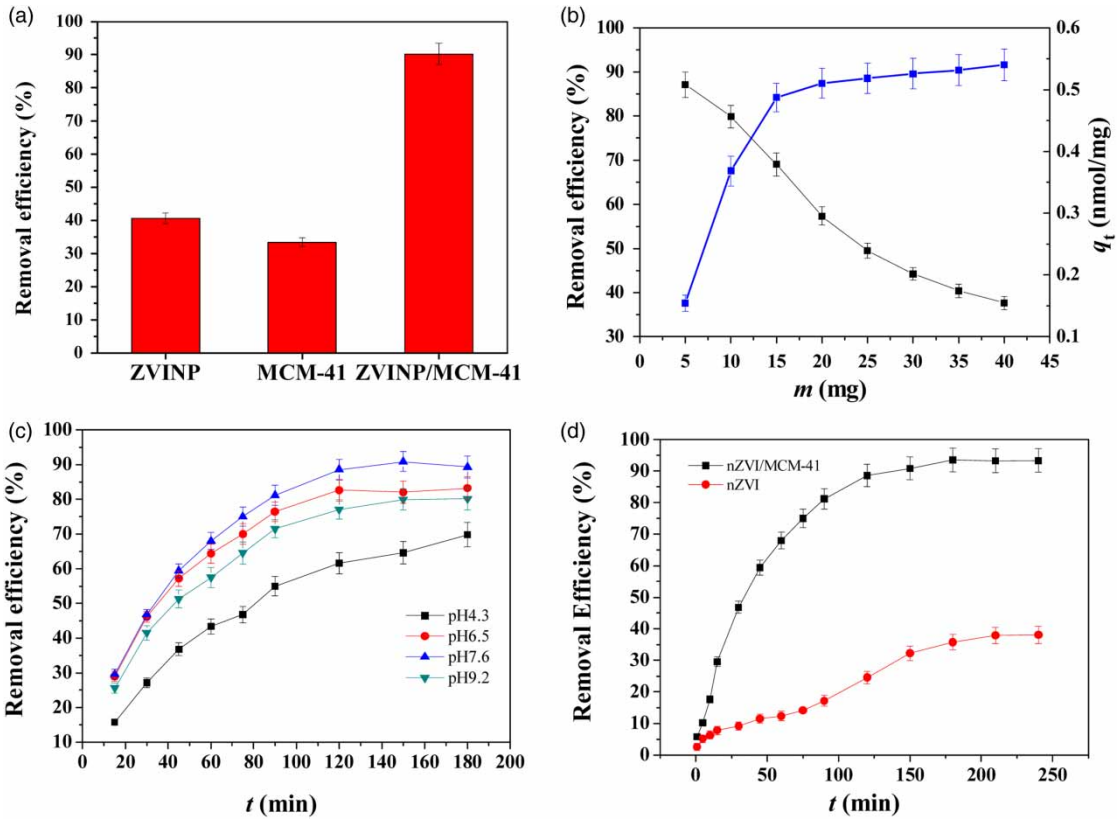

Figure 2 | Removal efficiencies of materials: (a) ZVINP, MCM-41, and ZVINP/MCM-41; (b) ZVINP/MCM-41 dose (5 to 40 mg); (c) initial pH (4.3 to 9.2); (d) and performing time (15–240 min). (All experiments under the conditions of 1,000 mL 1.0 μg/L NDMA solution at 25 °C.)

respectively. The results showed that the removal of NDMA by ZVINP/MCM-41 increased with time and reached equilibrium at about 2 h (Figure 2(d)).

In Figure 2(d), the removal efficiency of ZVINP was low in the first 90 min, increased after 90 min and got to equilibrium after 210 min, and it is also shown that the removal rate of ZVINP/MCM-41 was faster than ZVINP. Reaction kinetics were needed to confirm it.

Reaction kinetics

In order to investigate the mechanism of reduction and potential rate-limiting steps such as mass transport and chemical reduction reaction processes, the reaction time data of NDMA using ZVINP/MCM-41 and ZVINP were analyzed by kinetic models, such as the first-order kinetic model (Equation (3)), second-order kinetic model (Equation (4)), Elovich model (Equation (5)), and intraparticle diffusion model (Equation (6)). The results are calculated and shown in Figure 3 and Table 1. The measured kinetic data of NDMA removed by ZVINP/MCM-41 at pH 4.3, 6.5, 7.6 and 9.2 fitted the second-order kinetic model with a correlation coefficient (R^2) of 0.998, 0.999, 0.998 and 0.999. The linear plots of $1/q_t$ versus $1/t$ show good agreement between experimental values (q_e(exp)) and (q_e(cal)), where q_e (μg/g) is the removal amount at equilibrium. It suggested that the removal process could be a rate-limiting step (Ho 2006).

$$\ln(q_e - q_t) = \ln q_e - k_1 t \tag{3}$$

$$\frac{1}{q_t} = \frac{1}{q_e^2 k_2} \cdot \frac{1}{t} + \frac{1}{q_e} \tag{4}$$

$$q_t = \left(\frac{1}{\beta}\right) \ln(\alpha\beta) + \left(\frac{1}{\beta}\right) \ln t \tag{5}$$

$$q_t = k_p t^{1/2} + C \tag{6}$$

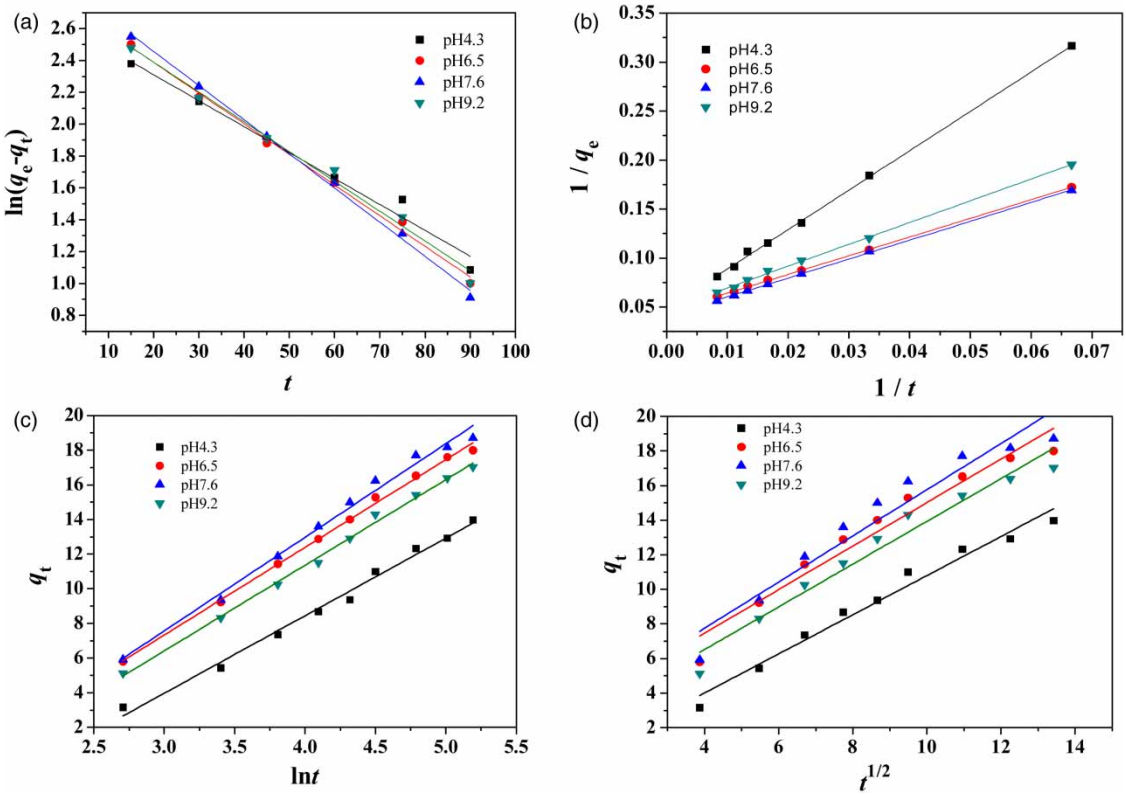

Figure 3 | (a) First-order kinetics, (b) second-order kinetics, (c) Elovich model and (d) intraparticle diffusion model fit of NDMA removal on ZVINP/MCM-41 at different pH (15–240 min removal experiments were carried out at 25 °C for the removal of 1,000 mL 1.0 μg/L NDMA solution onto 20 mg ZVINP/MCM-41).

Table 1 | Constants and correlation coefficients for the kinetic models

Model	Parameter	pH 4.3	pH 6.5	pH 7.6	pH 9.2
First-order model	q_e(μg/g)	13.96	15.99	17.92	15.85
	k_1 (min^{-1})	0.0163	0.0192	0.0214	0.0187
	R^2	0.976	0.994	0.996	0.986
Second-order model	q_e(μg/g)	20.37	22.32	24.04	21.37
	k_2(μg/(g min))	0.012	0.023	0.022	0.020
	R^2	0.998	0.999	0.998	0.999
Elovich model	β(g/μg)	0.223	0.198	0.185	0.202
	α(μg/(g min))	0.541	1.073	1.092	0.901
	R^2	0.989	0.997	0.986	0.996
Intraparticle diffusion model	C	0.526	2.427	2.403	1.567
	k_p	1.132	1.259	1.336	1.236
	R^2	0.974	0.945	0.926	0.957

Rate constants (k_2) of ZVINP/MCM-41 at pH 4.3, 6.5, 7.6 and 9.2 were 0.012 g μg^{-1} min^{-1}, 0.023 g μg^{-1} min^{-1}, 0.022 g μg^{-1} min^{-1} and 0.020 g μg^{-1} min^{-1}, respectively. The results showed that the reduction process of ZVINP/MCM-41 under neutral or weak acid conditions was faster than that under acidic or alkaline conditions. In addition, the removal capacity under neutral or weak acid conditions was larger than that under acidic or alkaline

conditions. NDMA can exist stably under acidic or alkaline conditions. The difference at different pH was due to the structure of ZVINP/MCM-41. Conditions that were too acidic or alkaline could change the ZVINP in ZVINP/MCM-41. Under acidic conditions, ZVINP could transfer to Fe^{3+} in solution, which reduced the ZVINP content of ZVINP/MCM-41. Under alkaline conditions, $Fe(OH)_3$ could be generated on the surface of ZVINP, which could block the reaction of ZVINP and NDMA.

Adsorption isotherms

The adsorption capacities of the as-obtained ZVINP/MCM-41 to NDMA were measured individually at pH 7.6 with 20 mg ZVINP/MCM-41 and varied NDMA concentration (1.0–6.0 μg/L). The Henry, Langmuir, and Freundlich models expressed in Equations (7)–(9) were used for modeling these adsorption isotherm data. All the isotherms showed a similar shape and were nonlinear over a wide range of aqueous equilibrium concentrations, shown in Figure 4.

$$q_e = kc_e \tag{7}$$

$$q_e = \frac{bq_m c_e}{1+bc_e} \quad \frac{1}{q_e} = \frac{1}{bq_m}\cdot\frac{1}{c}+\frac{1}{q_m} \tag{8}$$

$$q_e = K_F c_e^{1/n} \quad \ln q_e = \ln K_F + \frac{1}{n}\ln c_e \tag{9}$$

The fitted constants along with regression coefficients (R^2) are summarized in Table 2; q_m is the maximum adsorption capacity (μg/g). The data for NDMA adsorbed at equilibrium (q_e, μg/g) and the equilibrium metal concentration (c_e, μg/L) were fitted to the Langmuir adsorption model. The data fit well to the model with correlation coefficients (R^2) of 0.996. The Langmuir model is based on three assumptions: (1) the adsorption of molecules is a monolayer adsorption; (2) the adsorption on the adsorbent surface is uniform; (3) there is no interaction among adsorbed molecules. Therefore, the removal of NDMA onto ZVINP/MCM-41 is monolayer uniform adsorption. From Table 2, the calculated maximum adsorption capacity is 23.5 μg/g, which is in agreement with

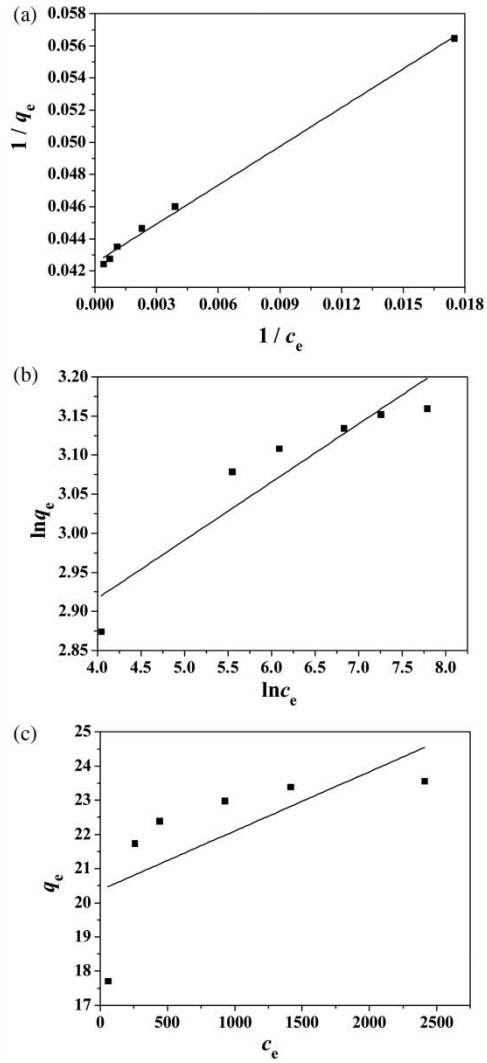

Figure 4 | (a) Langmuir, (b) Freundlich, and (c) Henry adsorption isotherm fits of NDMA removal on ZVINP/MCM-41.

Table 2 | Constants and correlation coefficients of adsorption isotherms

Model	Langmuir			Freundlich			Henry	
Parameter	q_m	B	R^2	K_F	n	R^2	K	R^2
Results	23.5 μg/g	0.053 L/μg	0.996	2.62	13.5	0.842	0.00173 L/g	0.356

the above-mentioned conclusion obtained from reaction kinetics.

NDMA reduction products and proposed mechanism

Figure 5 shows the products of NDMA reduction. At the first 30 minutes, the concentration of NDMA decreased, total nitrogen in the solution decreased, but UDMH and DMA were hardly found in the solution. It could be explained that at this stage adsorption was dominant. After that, the concentration of NDMA decreased with time, and UDMH and DMA could be detected in the solution. This showed that after 30 min, ZVINP in the ZVINP/MCM-41 began to play a role of reduction.

As NDMA degraded, DMA and UDMH formed accordingly. The nitrogen mass balance varied with the degradation of NDMA, and the final nitrogen mass balance was only 70.4%. UDMH accounted for 48.9% of the nitrogen mass, while DMA accounted for 21.5%. The loss of nitrogen mass was about 29.6%. The most detected products in the previous studies on NDMA reduction have been DMA and ammonium (NH_4^+) (Davie *et al.* 2008; Frierdich *et al.* 2009). This can explain some nitrogen loss. Others may be adsorbed into ZVINP/MCM-41.

From the whole process we could infer that the removal of NDMA from water involves three main steps: (1) ZVINP/MCM-41 adsorbed NDMA onto the surface; (2) ZVINP/MCM-41 reduced NDMA to DMA and ammonium; (3) DMA was desorbed into the solution.

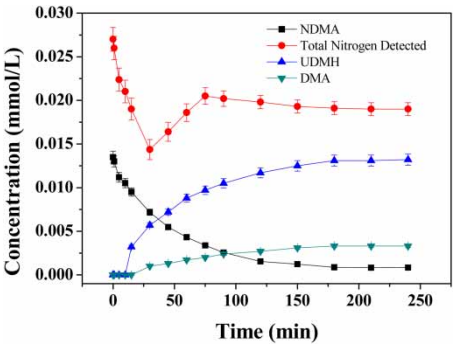

Figure 5 | Products of NDMA reduction with ZVINP/MCM-41 (0–240 min removal experiments were carried out at 25 °C for the removal of 1,000 mL 1.0 μg/L NDMA solution onto 20 mg ZVINP/MCM-41).

CONCLUSIONS

In the study, ZVINP/MCM-41 was prepared, and batch equilibrium removal of NDMA onto ZVINP/MCM-41 was carried out. Removal of the NDMA onto ZVINP/MCM-41 reached equilibrium within 120 min at pH 7.6, which agrees well with the second-order kinetic model. The product analysis found that in the process of removal, adsorption and reduction exist. Furthermore, the reduction reaction occurred after the adsorption reaction. It showed that this removal process was one of adsorption and reduction synergies.

ACKNOWLEDGEMENTS

This study was supported by National Major Projects on Water Pollution Control and Management Technology (No. 2012ZX07404-003) and the Natural Science Foundation of Shandong Province (No. ZR2014EEP008).

REFERENCES

Andrzejewski, P., Kasprzyk-Hordern, B. & Nawrocki, J. 2008 *N*-nitrosodimethylamine (NDMA) formation during ozonation of dimethylamine-containing waters. *Water Research* **42** (4–5), 863–870.

Choi, J. H. & Valentine, R. L. 2002 Formation of *N*-nitrosodimethylamine (NDMA) from reaction of monochloramine: a new disinfection by-product. *Water Research* **36** (4), 817–824.

Chun, C. L., Baer, D. R., Matson, D. W., Amonette, J. E. & Penn, R. L. 2010 Characterization and reactivity of iron nanoparticles prepared with added Cu, Pd and Ni. *Environmental Science and Technology* **44**, 5079–5085.

Davie, M. G., Shih, K., Pacheco, F. A., Leckie, J. O. & Reinhard, M. 2008 Palladium–indium catalyzed reduction of *N*-nitrosodimethylamine: indium as a promoter metal. *Environmental Science and Technology* **42** (8), 3040–3046.

Dimos, K., Stathi, P., Karakassides, M. A. & Deligiannakis, Y. 2009 Synthesis and characterization of hybrid MCM-41 materials for heavy metal adsorption. *Micro. Meso. Mater.* **126**, 65–71.

Fan, J., Shui, W. Q., Yang, P. Y., Wang, X. Y., Xu, Y. M., Wang, H. H., Chen, X. & Zhao, D. Y. 2005 Mesoporous silica nanoreactors for highly efficient proteolysis. *Chem.-Eur. J.* **11**, 5391–5396.

Frierdich, A. J., Joseph, C. E. & Strathmann, T. J. 2009 Catalytic reduction of *N*-nitrosodimethylamine with nanophase nickel–boron. *Applied Catalysis B: Environmental* **90** (1–2), 175–183.

Han, Y., Chen, Z., Tong, L., Yang, L., Shen, J., Wang, B., Liu, Y., Liu, Y. & Chen, Q. 2013 Reduction of *N*-nitrosodimethylamine with zero-valent zinc. *Water Research* **47**, 216–224.

He, F. & Zhao, D. Y. 2005 Preparation and characterization of a new class of starch-stabilized bimetallic nanoparticles for degradation of chlorinated hydrocarbons in water. *Environmental Science and Technology* **39**, 3314–3320.

Ho, Y. S. 2006 Review of second-order models for adsorption systems. *J. Hazard. Mater.* **136**, 681–689.

Li, Y., Zhang, Y., Li, J. & Zheng, X. 2011 Enhanced removal of pentachlorophenol by a novel composite: nanoscale zero valent iron immobilized on organobentonite. *Environ. Pollut.* **159**, 3744–3749.

Liu, H., Li, Y., Wu, H., Yang, W. & He, D. 2014 Promoting effect of glucose and *β*-cyclodextrin on Ni dispersion of Ni/MCM-41 catalysts for carbon dioxide reforming of methane to syngas. *Fuel* **136**, 19–24.

Lv, X. S., Xu, J., Jiang, G. M. & Xu, X. H. 2011 Removal of chromium(VI) from wastewater by nanoscale zero-valent iron particles supported on multiwalled carbon nanotubes. *Chemosphere* **85**, 1204–1209.

Mitch, W. A. & Sedlak, D. L. 2002 Formation of *N*-nitrosodimethylamine (NDMA) from dimethylamine during chlorination. *Environmental Science and Technology* **36** (4), 588–595.

Mitch, W. A., Sharp, J. O., Trussell, R. R., Valentine, R. L., Alvarez-Cohen, L. & Sedlak, D. L. 2003 *N*-Nitrosodimethylamine (NDMA) as a drinking water contaminant: a review. *Environmental Engineering Science* **20** (5), 389–404.

Odziemkowski, M. S., Gui, L. & Gillham, R. W. 2000 Reduction of *N*-nitrosodimethylamine with granular iron and nickel-enhanced iron. 2. Mechanistic studies. *Environmental Science and Technology* **34** (16), 3495–3500.

Phenrat, T., Saleh, N., Sirk, K., Tilton, R. D. & Lowry, G. V. 2006 Aggregation and sedimentation of aqueous nanoscale zerovalent iron dispersions. *Environmental Science and Technology* **41**, 284–290.

von Gunten, U., Salhi, E., Schmidt, C. K. & Arnold, W. A. 2010 Kinetics and mechanisms of *N*-nitrosodimethylamine formation upon ozonation of *N*,*N*-dimethylsulfamide-containing waters: bromide catalysis. *Environmental Science and Technology* **44** (15), 5762–5768.

Wakayama, H., Setoyama, N. & Fukushima, Y. 2003 Size-controlled synthesis and catalytic performance of Pt nanoparticles in micro- and mesoporous silica prepared using supercritical solvents. *Advanced Materials* **15**, 742–745.

Wang, W., Zhou, M., Jin, Z. & Li, T. 2010 Reactivity characteristics of poly(methyl methacrylate) coated nanoscale iron particles for trichloroethylene remediation. *J. Hazard. Mater.* **173**, 724–730.

Yang, L., Chen, Z. L., Shen, J. M., Xu, Z. Z., Liang, H., Tian, J. Y., Ben, Y., Zhai, X., Shi, W. X. & Li, G. B. 2009 Reinvestigation of the nitrosamine-formation mechanism during ozonation. *Environmental Science and Technology* **43** (14), 5481–5487.

Yang, L., Chen, Z. L., Shen, J. M., Liu, X. W., Li, H. Y. & Han, Y. 2010 Improved method for determining trace dimethylamine in water by gas chromatography. *China Water & Wastewater* **26** (8), 93–97.

Zhang, Y., Li, Y., Li, J., Hu, L. & Zheng, X. 2011 Enhanced removal of nitrate by a novel composite: nanoscale zero valent iron supported on pillared clay. *Chemical Engineering Journal* **171**, 526–531.

First received 20 April 2016; accepted in revised form 19 December 2016. Available online 23 January 2017